PCCP

Accepted Manuscript

This is an *Accepted Manuscript*, which has been through the Royal Society of Chemistry peer review process and has been accepted for publication.

Accepted Manuscripts are published online shortly after acceptance, before technical editing, formatting and proof reading. Using this free service, authors can make their results available to the community, in citable form, before we publish the edited article. We will replace this *Accepted Manuscript* with the edited and formatted *Advance Article* as soon as it is available.

You can find more information about *Accepted Manuscripts* in the **Information for Authors**.

Please note that technical editing may introduce minor changes to the text and/or graphics, which may alter content. The journal's standard **Terms & Conditions** and the **Ethical guidelines** still apply. In no event shall the Royal Society of Chemistry be held responsible for any errors or omissions in this *Accepted Manuscript* or any consequences arising from the use of any information it contains.

Theoretical Studies on the Carrier Tunability of Oxidized Oligothiophenes

Anup Pramanik and Pranab Sarkar[*]

Department of Chemistry, Visva-Bharati University, Santiniketan- 731235, India

E-mail: pranab.sarkar@visva-bharati.ac.in

Abstract

A first principle density functional theory calculation in combination with non-equilibrium Green's function technique has been performed to show the carrier tunability of a family of thiophene-1,1-dioxide (TDO) oligomers. Our theoretical results interpret how the molecular length dictates the nature of charge carrier that has very recently been observed through thermopower measurement (Nat. Chem., DOI: 10.1038/NCHEM.2160). Our molecular level understanding dictates that with increasing the conjugation length through molecular backbone, it is the LUMO orbital which is stabilized more and thus participates in resonance tunneling with the gold electrode. Thus HOMO resonating channel, which is the major transporting channel for TDO1, is shifted to LUMO resonating channel in case of TDO4. This carrier switching from hole to electron is unique for these type of organic materials.

---
[*]To whom correspondence should be addressed

Introduction

The solution processability and modular structure of conjugated organic molecules specially make them attractive for use in elctronics devices like photovoltaics, light-emitting diodes, field effect transistors, etc.[1–4] Tunable electronic properties of such semiconducting organic molecules are the guiding factors for molecular electronics where a single molecule is the key for electronic circuit. The precise control afforded over molecular design by the use of sophisticated organic synthetic methodologies allows device properties to be tuned readily. The basis of these electronics devices is the single molecular junction. So, precise knowledge over the junction processes and the nature of charge transport will have immense importance on device fabrication. Semiconducting organic molecules are of two types, hole transporting (p-type) and electron transporting (n-type). Most of the organics electronics are composed of p-type materials.[5] This is because of the fact that hole transporting materials have higher charge mobility and these are more stable in ambient conditions.[2] However, stable n-type organic semiconductors are required for designing efficient complementary logic circuit.[6] Design principles to create stable n-type organic materials are now evolving. The most successful strategy for converting p-type oligothiophenes into n-type materials was the insertion of thiophene-1,1-dioxide (TDO) moieties into oligothiophene backbone.[7] This oxidation causes the thiophene ring to lose aromaticity, while inserting a strong electron-withdrawing group lowers the lowest unoccupied molecular orbital (LUMO).[8] It has been demonstrated that this lowering of LUMO is the key factor for this carrier switching phenomenon. However, the point at which this carrier switching occurs is really an ambiguous question.[9,10]

From the synthetic point of view it is a big challenge to synthesis and characterize the n-type semiconductor since families of n-type materials are underdeveloped in comparison to their p-type counterparts. Furthermore, identifying the crossover point of carrier switching is of fundamental importance for designing and developing advanced organic electronics materials. However, to characterize the carrier type one has to design proper molecular contact, as because molecular conductance depends on the intra and intermolecular coupling scheme.[11–17] Modern sophisticated techniques such as scanning tunneling microscopy (STM), atomic force microscopy (AFM) along

with the molecular break junction (BJ) method, however, have been successfully utilized to fabricate metal-molecule-metal contact through selective site attachment.[18–20] In STM-BJ technique, a molecule is bridged in between two nanoscale gold electrodes and its conductance is measured. The conductance depends on the energetic alignment of the frontier molecular orbitals with the Fermi level of the metal (in most cases, gold) electrodes. It is worth mentioning that, the molecular transport is characterized as "electron transport" ("hole transport") if the conduction is mediated by tunneling through the LUMO (HOMO).[21] Thus, it requires a deep theoretical understanding on the electronic structure of the molecule and the metal-molecule contact to characterize the nature of charge carrier.

The purpose of this communication is to give a physical account on the transport characteristics of the TDO oligomers which have recently been characterized.[9] Although some low-level computations have already been done, further details are required to properly locate the resonance transmission channels in order to address the carrier switching behavior. On the basis of abinitio quantum mechanical studies we will show how length of molecular backbone controls the position of LUMO orbital thereby dictating the nature of charge carrier.

Model and method of calculation

For modeling, we fist choose the trithiophene molecule and its oxidized counterpart where the middle ring of the trithiophene was replaced by TDO moiety. The higher oligomers were designed by incorporating more TDO units. Thus the oxidized thiophenes (TDOn) reefer to n number of TDO unit conjugated through two thiophene units at both ends (please see Fig. 1). As a computational strategy, we searched for the ground state optimized geometry using different basis set and exchange correlation functional in the framework of density functional theory (DFT).[22] Although DFT underestimates LUMO energy, the use of hybrid functional solves this discrepancy within a reasonable accuracy. Thus, we adopted hybrid functionals like B3LYP, HSE06 for calcu-

lating the HOMO-LUMO gap of the molecules.[23] All the calculations were done using Gaussian 09 program suite.[24] We find that HSE06/6311G* fits best (default for presenting results here for free molecule) for mimicking the HOMO-LUMO gap of the oligothiophenes as estimated from CV measurement,[9] and these optimized geometries were then used for next step transport calculations.

Based on the optimized geometries of the molecules we then performed time dependent DFT (TD-DFT) calculations to compute the UV-vis spectra in dichloromethane (DCM) solvent. We adopted the most suitable hybrid function and the basis set (HSE06/6311G*) and the computations in DCM were performed by applying self-consistent reaction field method within isodensity model (IPCM)[25] as implemented in Gaussian 09.[24] The absorption spectra were simulated by using the 20 lowest spin-allowed singlet transitions, and finally the spectral data were plotted using mixed Lorentziane Gaussian lineshape (0.5) and an average full-width at the half maximum (3000 cm^{-1}) for all peaks.

In order to model different metal-molecule-metal contact moiety, as a common strategy, we choose Au(111)-3×3 surface as electrode.[17,26,27] It is well known that the binding energy of small molecules to Au(111) surface is larger than that of other surfaces like Au(001), etc.[17] Moreover, energy differences between different adsorption sites of Au(111) surface are relatively lower. Thus we choose Au(111) surface as contact lead. As shown in Fig. 1, both the electrodes are defined by three layered unit cells of Au(111) surface. The scattering unit is formed by the oligothiophene molecule with an additional two-layered Au surface thereby establishing a common Fermi energy for the electrode and the scattering region. As could be found from Fig. 1, the oligothiophenes are functionalized with -SMe groups at the both ends. To mimic the STM-BJ experimental contact configuration[9,10] we added an extra Au atom to both of the S atoms of the -SMe groups. Finally, the molecule was placed in between the two leads such that the extra Au atoms are placed at the center of the triangular arrangement of the Au(111) surface maintaining the optimized Au-Au distance of 2.9 Å. The molecules were then allowed to relax keeping atomic positions of both the electrodes into fixed. Thus, we computed the crude binding energies which are in between 3.5 to 4.3 eV for TDO1-4 and are in line with those of small molecules in unrelaxed situation as reported earlier.[17]

4

The transport properties are calculated using TranSIESTA module within the SIESTA package,[28] which is based on the combination of density functional theory and non-equilibrium Green's function method.[29,30] The non-equilibrium Greens function (NEGF) formalism has been employed in this two probe model for calculating tunneling current using Landauer-Buttiker formula,

$$I(V_b) = \frac{2e}{h} \int_{-\mu_L}^{\mu_R} T(E,V_b)[f_L(E-\mu_L) - f_R(E-\mu_R)]dE \tag{1}$$

where $f_{L(R)}$ is the Fermi-Dirac distribution function for left (right) electrode, and $\mu_{L(R)}$ is the electrochemical potential of the left (right) electrode such that at a finite bias V_b, $eV_b = \mu_L - \mu_R$. The bias dependent transmittance, $T(E,V_b)$ of an incident electron with energy E is given by

$$T(E,V_b) = Tr[\Gamma_L G^R \Gamma_R G^A] \tag{2}$$

where $G^{R(A)}$ is the retarded (advanced) Green's function of the scattering region, and $\Gamma_{L(R)}$ is the coupling strength of the left (right) electrode. We wish to mention here that the pseudo Fermi level is determined as a consequence of self-consistence process. As implemented in TranSIESTA code, the energy scale is shifted so that at zero bias condition the Fermi level of the system is set to zero. So, the zero-bias transmittance at the Fermi level is then given by T(E=0). When there is a finite bias (V_b), the Fermi energy of the left electrode is placed at $V_b/2$, and that of the right electrode at $-V_b/2$. We employed double-ζ plus polarization function (DZP) basis set for all the atom except Au, for which single-ζ with polarization function (SZP) basis set was used. Norm-conservative Troullier- Martins pseudo-potentials (PP)[31] were used for representing the valence and inner electrons, and a real space mesh cutoff of 250 Ry has been used throughout the entire calculation. The exchange-correlation functional of the generalized gradient approximation is represented by the Perdew-Burke-Ernzerhof approximation.[32] The convergence criteria for the density matrix is taken as 10^{-4}. The conjugate gradient method is used to relax all the atoms until the maximum absolute force was less than 0.005 eV/Å. We have used finite bias from -3 V to 3V with small grid of 0.1 V to investigate the current-voltage (I-V) characteristic of the molecular contacts.

Results and discussion

Let us first check the optoelectronic properties of the molecules. In order to check the molecular orbital alignment we performed a series of DFT calculations with different exchange correlation functionals and basis sets and the results are summarized in Table 1. Thiophene-1,1-dioxide (TDO), an oxidized counterpart of thiophene, imparts different electronic properties as because the lone pairs on S atom are involved in the bonding interactions with O and are no longer available for aromatic delocalization with the thiophene ring. Thus, when middle ring of trithiophene (T3) is oxidized, the HOMO-LUMO gap of it is reduced from 2.92 eV to 2.23 eV, while for fully oxidized case the same is further reduced to 1.98 eV. This is also reflected from the computed absorption maxima of the substances. The fully unoxidized trimer (T3) shows an absorption maximum at 457 nm in dichloromethane (DCM) solvent, while dioxygenation at the middle ring leads to a redshifting of about 88 nm. Furthermore, the fully oxidized thiophene trimer shows a λ_{max} in the same solvent at 597 nm. Most importantly, with increasing degree of oxygenation the delocalization in the LUMO orbital increases as shown in Fig. 2 and thus it lowers the energy of LUMO orbital. Thus, dioxygenation of oligothiophene leads to oligoene type of backbone with electron deficiency. However, with increasing the length of the oligomer, the optical gap decreases, as also be observed from the red-shift in their UV-vis spectra. Our computed UV-vis spectra in DCM are in well agreement with the experimental observations.[9] The major cause of this red-shift is attributed to the relative lowering of the LUMO level while the shifting of HOMO level is relatively lower.

Fig. 3 gives the computed UV-vis spectra of the oligomers. As indicated from the figure, the maximum absorption wavelength for TDO1 is observed at 546 nm. This is in excellent agreement with the experimentally observed longest onset wavelength of 575 nm.[9] With increasing the TDO unit not only the λ_{max} increases, but the intensity of absorption also increases, however, the peak is broadened. Now, what actually happens with increasing the number of TDO unit is that, the

increased conjugation in the oligoene type of backbone leads to the lowering of LUMO level as already stated. This can be inferred from the fact that, the HOMO of the DTO molecules (please see Fig. 4) are associated with the C-C bonds within a thiophene or oxidized thiophene ring which are hardly affected by the extent of conjugation. On the other hand, the LUMOs are involved in inter-ring C-C bond which is sensitive to conjugation length. Thus, with increasing the TDO units and hence conjugation length, the LUMO orbitals are stabilized. Thus, our simple DFT calculations give a theoretical basis of the observed cyclic voltametric results of Dell et al.[9] who report the oxidation peaks for the TDOn family at around the same position, while the reductions peaks of the same are shifted to the lower energy region. As could be seen from Table 1, the HOMO-LUMO gap of the TDO molecules in the HSE06/6311G* level of theory are in outstanding agreement with results obtained from CV measurements. The low reduction potential of the oxidized oligothiophene molecules could, however, be implied as the n-type of behavior of them, i.e. the higher oligomers are suspected as the LUMO conducting materials. In the subsequent section we will focus on the nonequilibrium electron transport phenomena of the oligothiophenes. Now returning to the spectral broadening issue, it may be understood on the basis of the following points. Firstly, with increasing the conjugation of the oligomer more similar states are introduced in the nearby region of the occupied and unoccupied states. That may also be inferred from the broadening of the DOS peaks. Secondly, the closeness of the HOMO and the HOMO-1 states also leads to additional broadening of the HOMO related DOS peak. Thus, the combined effect is supposed to cause the spectral broadening especially for the higher oligomers.

To test the transport characteristics of the oligothiophenes we imply two prob model as already discussed. For comparison we have plotted the current-voltage (I-V) characteristics of the TDO1-4 molecules in Fig. 5. The computed I-V characteristics look symmetrical as also reported in very recent experiment by Capozzi et al.[10] when studied in nonpolar solvent. The authors, however, report unsymmetrical I-V characteristics in a polar solvent, propylene carbonate (PC) due to formation of asymmetric double layer around the tip and the substrate region. The symmetric I-V characteristics are very common for these types of symmetrically substituted molecules.[27] In or-

der to have a deeper insight on the transport characteristics, we present zero bias transmittance as a function of relative energy in Fig. 6. The right panel of the same figure gives the projected density of states (PDOS) of the molecules. The figure reveals a one to one correspondence between the DOS peaks and the corresponding transmission peaks. At zero bias, as the Fermi energy of the electrode (here Au-111 surface) is set to zero, the first two DOS peaks at negative and positive region of Fermi energy correspond to the HOMO and LUMO of the molecule, respectively. Similarly, the transmission peaks at the similar positions correspond to the HOMO and LUMO resonance peaks, respectively. However, due to electrode-molecule interactions the transmission peak are redistributed, and even some low intensity peaks are appeared in between the transport gap region. These are referred to the metal induced transmission channels which serve important contribution in the low-bias transport properties of the molecular contact.[8,33] For TDO1, the HOMO resonance peak is broadened due to its interaction with the closely lying HOMO-1 channel. On the other hand, the sharp feature of the LUMO resonance peak indicates that the LUMO state is isolated. The peak centers of these two peaks are situated at -0.87, and 0.92 eV, respectively. These two peaks can be compared to the corresponding HOMO and LUMO density of states at -0.78 and 0.91 eV, respectively. It is noteworthy to mention here that, as the HOMO resonance peak is closer to the electrode-Fermi energy than the LUMO resonance peak, the transport can be characterized as HOMO-induced transport or hole transport. Thus, TDO1 is designated as hole transporting material. The transport characteristic may further be analyzed on the basis of molecular projected self-consistence Hamiltonian (MPSH) eigen-state analysis. We will show that MPSH-HOMO is crucially composed of the HOMO of TDO1. This theoretical analysis is in accordance with the Seebeck measurement on TDO1, which gives positive Seebeck coefficient.[9] We wish to mention here that, the transport characteristics of the unoxidized T3 molecule is also similar as could be seen from Fig. 6.

In contrast, for TDO4, the measured Seebeck coefficient is negative as reported by Dell et al.[9] We can, of course, understand this phenomenon on the basis of the relative position of the HOMO and LUMO resonating peaks in the transmission plot. It is evidenced that with increasing delo-

calization in the polyene-type of backbone the LUMO state approaches towards the more negative energy region that has already been discussed. Now this enforces the appearance of LUMO resonating peak closer to the electrode Fermi level. That actually happens in case of TDO4. Fig. 6 depicts that the LUMO resonating peak for TDO4 is centered at 0.41 eV, while the HOMO resonating peak is originated at -0.62 eV. Obviously, TDO4 is to be considered as LUMO conducting or electron conducting material which must show negative Seebeck coefficient. For other two oligothiophenes, TDO2 and TDO3 the situation is much more complicated and it is little bit difficult to predict the nature of charge carrier from the calculated transmission spectra value. However, we may assert that, during the increase in the length of the oligothiophene backbone there occurs a clear switching of charge carrier from hole to electron. The actual length at which the switching occurs, we can not predict, but our theoretical analysis certainly proves the conductance switching in between TDO1 and TDO4 that has recently been speculated on the basis of thermoelectric measurement.[9] It is noteworthy to mention here that although the electronic properties of the molecules are best reproduced using hybrid functionals like HSE06, for transport calculation we adopted PBE exchange correlation only. However, still we believe that the results of our transport calculation within GGA/PBE is reproducible, at least from the qualitative point of view, since both the electrode and the molecular properties are calculated in the same level of theory. Thus, the relative position of the frontier energy levels and their sequences will not be altered so much.

For applicability of such systems, we must study the transport characteristics at finite bias. As could be seen from Fig. 7, the transmission spectra at $V_b = 1$ V for the TDOn oligomers look similar to those at zero bias. One change which is easily recognizable is that, the transmittance values of LUMO resonating peaks for TDO2-4 are reduced by half. Secondly and most importantly, although the projected density of states are almost zero at Fermi energy, there appear low intensity transmission peaks there. These are referred as edge induced transmission channels. At finite bias $V_b = 1$ V, the bias window is defined as ± 0.5 V. Thus the current would be calculated by integrating the transmittance within this bias window. Fig. 7 clearly indicated that, within the bias window ± 0.5 V, the edge induced transmission channels contribute for current for all the

9

molecules TDO1-4, however the LUMO resonating transmission peaks additionally contribute for TDO3 and TDO4. So, it is speculated that TDO3 and TDO4 would show more current at V_b= 1 V than the others and that is really reflected from the I-V characteristics as shown in Fig. 5. At this end, we further demonstrate that at V_b= 1 V, the edge induced transmission peak is closely related to the HOMO resonating transmission peak. Thus a clear distinction between the carrier type for TDO1 and TDO3 or 4 is observed. However, With increasing the applied bias, more and more resonating channels enter into the bias window which subsequently increase the current.

In order to have a more clear picture on the resonance tunneling channels we present the isosurface plots of the MPSH states in Fig. 8 which are the renormalized eigenstates obtained by diagonalizing the self-consistence Hamiltonian of the molecular junction projected over the molecule. It is revealed that the main transporting channel, MPSH HOMO for TDO1 molecular junction is constituted by the HOMO of the TDO1 molecule. This ensures that molecular HOMO is the closest transporting channel for TDO1, i.e. TDO1 is hole transporting material. In sharp contrast, for TDO4, the molecular LUMO oriented MPSH state is the main transporting channel indicating TDO4 as electron conducting material. The situation for TDO3 resembles that of TDO4, but it is still ambiguous for TDO2. So, we may conclude that crossover point of carrier switching is in between TDO2 and TDO3.

Conclusion

In conclusion, we have given a physical insight on the length dependent carrier switching property of oxidized oligothiophenes on the basis of computational results obtained from density functional theory and non equilibrium Green's function method. We observe that with increasing conjugation in the polyene type of backbone of the TDO molecules, the LUMO energy is shifted towards lower value which enforces easier way of electron tunneling from metal electrode to the molecule via LUMO orbital. Thus unlike unoxidized oligothiophenes or lower member of oxidized oligothiophenes, higher members show electron conducting phenomena which is rare in these types

of organic molecules. Our computational result matches well with the observed optical band gap from CV experiments, which validates the level of accuracy of our calculations. The position of resonance transmission peak and the calculated MPSH eigen states support the understanding of the carrier type of the molecules.

Acknowledgment

References

(1) C. Wang, H. Dong, W. Hu, Y. Liu and D. Zhu, *Chemical Reviews*, 2011, **112**, 2208–2267.

(2) C.-H. Tsai, D. N. Chirdon, A. B. Maurer, S. Bernhard and K. J. Noonan, *Organic Letters*, 2013, **15**, 5230–5233.

(3) J. Shinar and V. Savvateev, *Introduction to organic light-emitting devices*, Springer, 2004.

(4) J. Mei, Y. Diao, A. L. Appleton, L. Fang and Z. Bao, *Journal of the American Chemical Society*, 2013, **135**, 6724–6746.

(5) I. Osaka, R. Zhang, G. Sauvé, D.-M. Smilgies, T. Kowalewski and R. D. McCullough, *Journal of the American Chemical Society*, 2009, **131**, 2521–2529.

(6) J. E. Cochran, E. Amir, K. Sivanandan, S.-Y. Ku, J. H. Seo, B. A. Collins, J. R. Tumbleston, M. F. Toney, H. Ade, C. J. Hawker *et al.*, *Journal of Polymer Science Part B: Polymer Physics*, 2013, **51**, 48–56.

(7) M. Melucci, P. Frere, M. Allain, E. Levillain, G. Barbarella and J. Roncali, *Tetrahedron*, 2007, **63**, 9774–9783.

(8) E. J. Dell and L. M. Campos, *J. Mater. Chem.*, 2012, **22**, 12945–12952.

(9) E. J. Dell, B. Capozzi, J. Xia, L. Venkataraman and L. M. Campos, *Nature Chemistry*, 2015, **7**, 209–214.

(10) B. Capozzi, J. Xia, O. Adak, E. J. Dell, Z.-F. Liu, J. C. Taylor, J. B. Neaton, L. M. Campos and L. Venkataraman, *Nature nanotechnology*, 2015.

(11) B. Zou, Z.-L. Li, X.-N. Song, Y. Luo and C.-K. Wang, *Chemical Physics Letters*, 2007, **447**, 69–73.

(12) Y. Luo, C.-K. Wang and Y. Fu, *The Journal of Chemical Physics*, 2002, **117**, 10283–10290.

(13) H. Kondo, H. Kino, J. Nara, T. Ozaki and T. Ohno, *Physical Review B*, 2006, **73**, 235323.

(14) K.-H. Müller, *Physical Review B*, 2006, **73**, 045403.

(15) Z.-L. Li, B. Zou, C.-K. Wang and Y. Luo, *Physical Review B*, 2006, **73**, 075326.

(16) M. Kula, J. Jiang, W. Lu and Y. Luo, *The Journal of Chemical Physics*, 2006, **125**, 194703.

(17) S.-H. Ke, H. U. Baranger and W. Yang, *Journal of the American Chemical Society*, 2004, **126**, 15897–15904.

(18) A. J. Simbeck, G. Qian, S. K. Nayak, G.-C. Wang and K. M. Lewis, *Surface Science*, 2012, **606**, 1412–1415.

(19) B. Xu and N. J. Tao, *Science*, 2003, **301**, 1221–1223.

(20) A. S. Blum, J. C. Yang, R. Shashidhar and B. Ratna, *Applied Physics Letters*, 2003, **82**, 3322–3324.

(21) Y. Xue and M. A. Ratner, *Physical Review B*, 2003, **68**, 115406.

(22) A. D. Becke, *The Journal of Chemical Physics*, 1993, **98**, 1372–1377.

(23) A. F. Izmaylov, G. E. Scuseria and M. J. Frisch, *The Journal of Chemical Physics*, 2006, **125**, 104103.

(24) M. J. Frisch *et al.*, *Gaussian 09 Revision D.01*, Gaussian Inc. Wallingford CT 2009.

(25) J. B. Foresman, T. A. Keith, K. B. Wiberg, J. Snoonian and M. J. Frisch, *The Journal of Physical Chemistry*, 1996, **100**, 16098–104.

(26) Z.-Q. Fan, K.-Q. Chen, Q. Wan and Y. Zhang, *Journal of Applied Phys*, 2010, **107**, 113713.

(27) S. Yuan, C. Dai, J. Weng, Q. Mei, Q. Ling, L. Wang and W. Huang, *The Journal of Physical Chemistry A*, 2011, **115**, 4535–4546.

(28) J. M. Soler, E. Artacho, J. D. Gale, A. García, J. Junquera, P. Ordejón and D. Sánchez-Portal, *Journal of Physics: Condensed Matter*, 2002, **14**, 2745.

(29) M. Brandbyge, J.-L. Mozos, P. Ordejón, J. Taylor and K. Stokbro, *Physical Review B*, 2002, **65**, 165401.

(30) S. Datta, *Electronic transport in mesoscopic systems*, Cambridge university press, 1997.

(31) N. Troullier and J. L. Martins, *Physical Review B*, 1991, **43**, 1993.

(32) J. P. Perdew, K. Burke and M. Ernzerhof, *Physical Review Letters*, 1996, **77**, 3865.

(33) A. Pramanik, B. Mandal, S. Sarkar and P. Sarkar, *Chemical Physics Letters*, 2014, **597**, 1–5.

Table 1: Calculate HOMO, LUMO energy (in eV) and their difference (Δ, in eV) of TDO1-4 molecules in various level of theory. The values in parenthesis are the experimentally observed HOMO-LUMO gap from CV measurement (Ref. 9).

Level of Theory	TDO1			TDO1			TDO1			TDO1		
	H	L	Δ	H	L	Δ	H	L	Δ	H	L	Δ
B3LYP/ 6311G*	-5.36	-2.71	2.65	-5.51	-3.30	2.21	-5.61	-3.67	1.94	-5.69	-3.94	1.75
HSE06/ 6311G*	-5.16	-2.93	2.23 (2.1)	-5.31	-3.53	1.78 (1.8)	-5.41	-3.90	1.51 (1.6)	-5.49	-4.17	1.32 (1.4)
GGA/ PBE	-3.91	-2.30	1.61	-3.99	-2.73	1.26	-3.93	-2.87	1.06	-3.96	-3.04	0.92
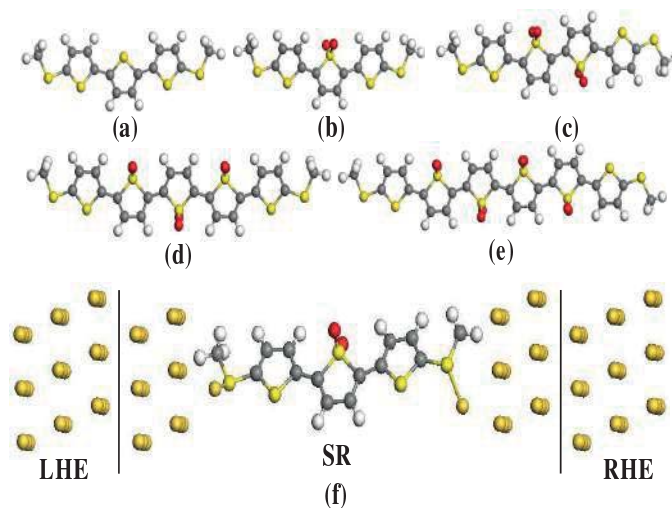
Figure 1: Optimized structures of reduced TDO1, i.e. T3 (a), TDO1-4 (b-e). Metal-Molecule-Metal contact geometry for transport calculation (f). Grey, white, red, yellow, and deep yellow colored balls represent C, H, O, S, Au atoms, respectively.
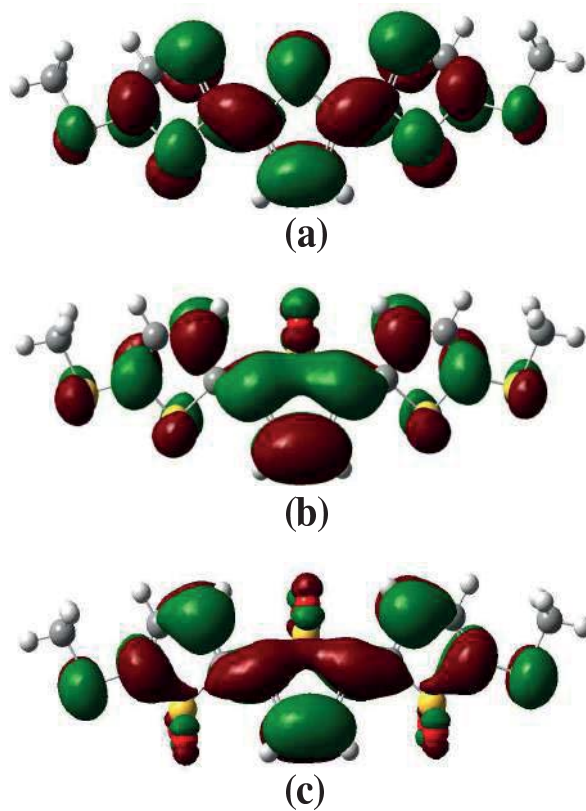
Figure 2: Computed LUMO isosurface plots of TDO1 (a), TDO2 (b), and TDO3 (c), respectively.
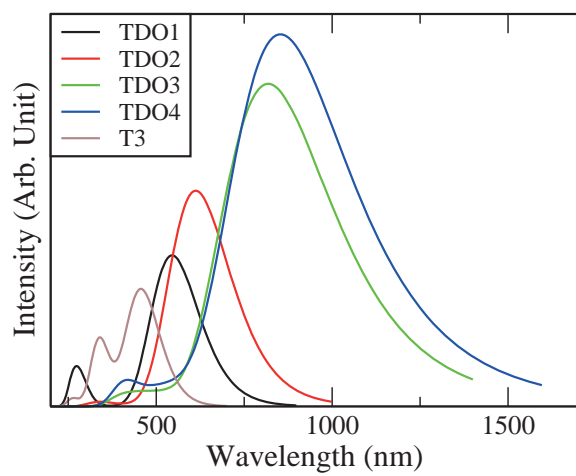
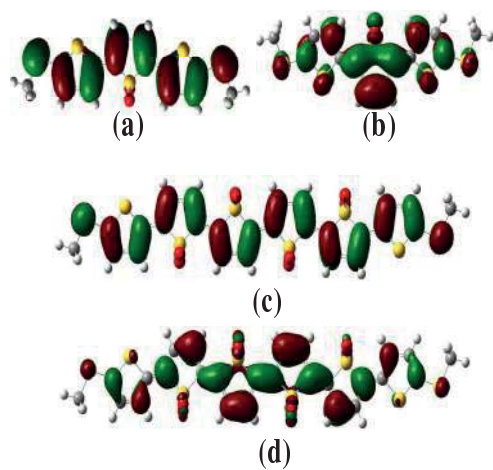Figure 3: Computed UV-vis spectra of the oxidized oligothiophenes (TDO1-4) in DCM solvent.

Figure 4: Computed HOMO (a, c) and LUMO (b, d) states of TDO1 and TDO4, respectively. Grey, white, red, and yellow colored balls represent C, H, O, S atoms, respectively.
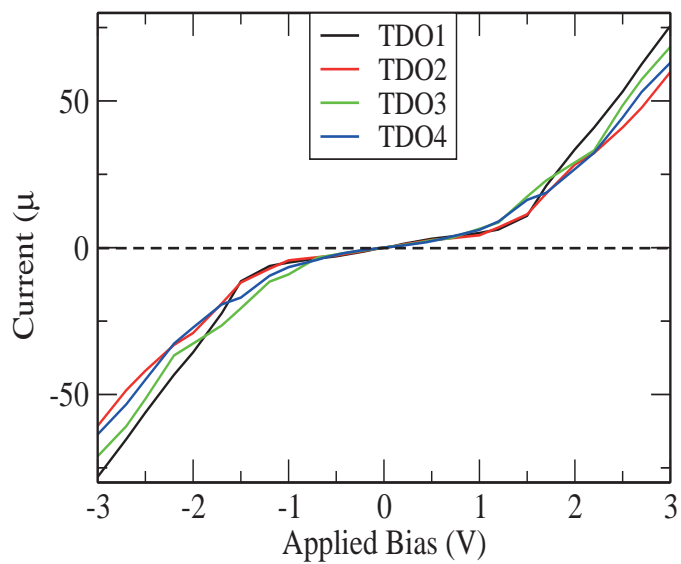
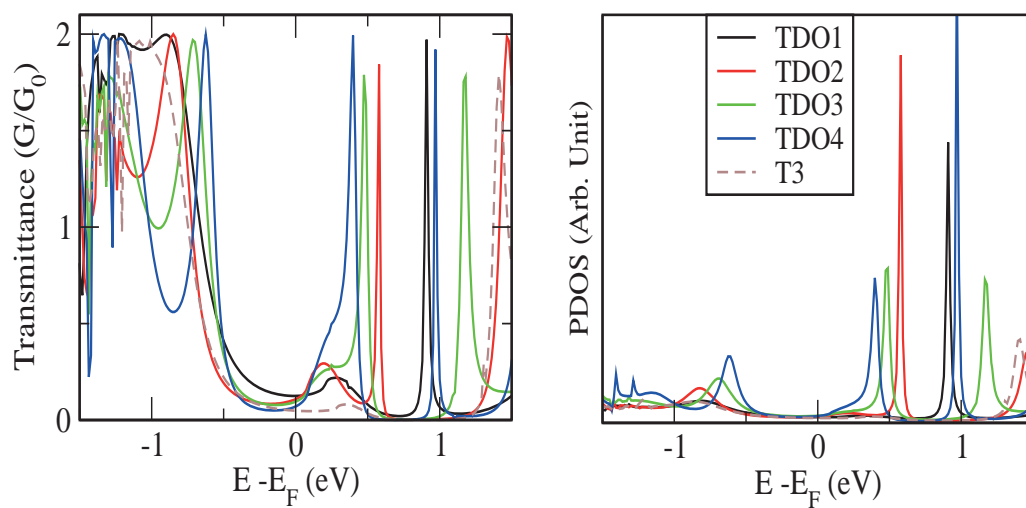Figure 5: Current-voltage characteristics of the oxidized oligothiophenes showing symmetric nature.

Figure 6: Zero-bias transmittance of TDO1-4 and T3 molecular junctions as a function of relative Fermi energy. The corresponding right panel shows Projected Density of States as a function of relative Fermi energy.
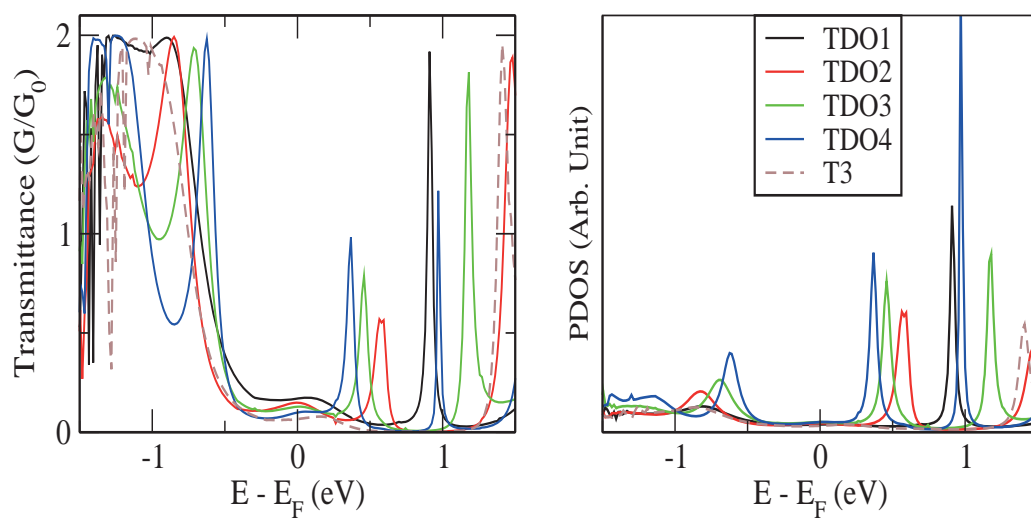
Figure 7: Finite-bias (V_b = 1.0 V) transmittance of TDO1-4 and T3 molecular junctions as a function of relative Fermi energy. The corresponding right panel shows Projected Density of States as a function of relative Fermi energy.
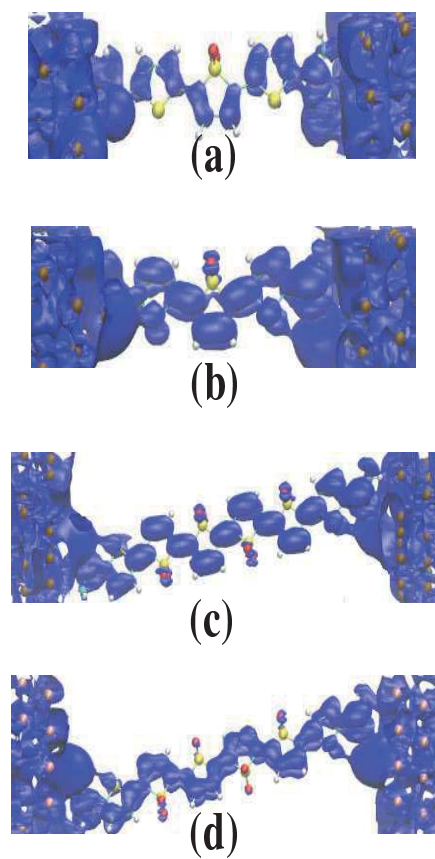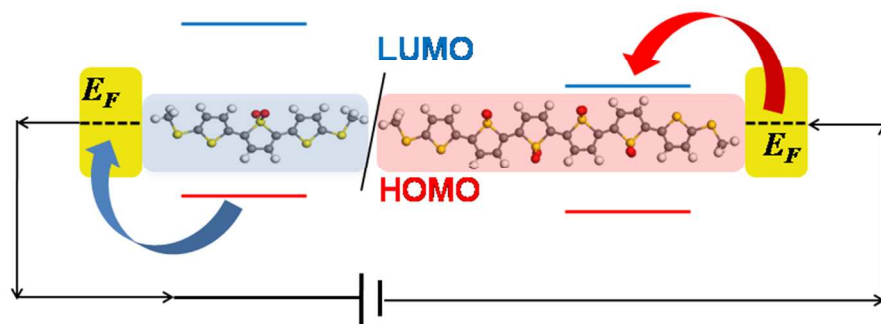
Figure 8: Isosurface plots of the MPSH eigenchannels in zero-bias condition for TDO1 (a-HOMO, b-LUMO) and TDO4 (c-HOMO, d-LUMO), respectively.

With increasing the molecular length hole conducting TDO1 is converted to electron conducting TDO4

254x190mm (96 x 96 DPI)